

# Study on the effect and mechanism of *Swertia mussoyii* Franch. in the treatment of primary biliary cholangitis based on bioinformatics and in vitro experiments

Xing-Fang Zhang<sup>1,2</sup>, Meng-Meng Yang<sup>1,2</sup>, Yi-Chen Guo<sup>1,3</sup>, Meng-Yuan Wang<sup>2</sup>, Hong-Xia Yang<sup>1,4</sup>, Ming Zhang<sup>1,4</sup>, Cen Li<sup>1,4</sup>, Li-Xin Wei<sup>1,4\*</sup>, Hong-Tao Bi<sup>1\*</sup>

<sup>1</sup>Qinghai Provincial Key Laboratory of Tibetan Medicine Pharmacology and Safety Evaluation, Northwest Institute of Plateau Biology, Chinese Academy of Science, Xining 810008, China. <sup>2</sup>Medical College, Qinghai University, Xining 810001, China. <sup>3</sup>College of Eco-Environmental Engineering, Qinghai University, Xining 810016, China. <sup>4</sup>CAS Key Laboratory of Tibetan Medicine Research, Northwest Institute of Plateau Biology, Chinese Academy of Sciences, Xining 810001, China.

\*Correspondence to: Hong-Tao Bi, Qinghai Provincial Key Laboratory of Tibetan Medicine Pharmacology and Safety Evaluation, Northwest Institute of Plateau Biology, Chinese Academy of Sciences, NO. 23 Xinning Road, Xining 810008, China. E-mail: [bihongtao@hotmail.com](mailto:bihongtao@hotmail.com); Li-Xin Wei, CAS Key Laboratory of Tibetan Medicine Research, Northwest Institute of Plateau Biology, Xining 810001, China. E-mail: [lxwei@nwipb.cas.cn](mailto:lxwei@nwipb.cas.cn).

## Author contributions

Zhang XF, Bi HT and Wei LX designed the study. Zhang XF, Yang MM, and Guo YC performed the experiments. Zhang XF, Yang MM, Guo YC, and Wang MY analyzed the data and wrote the manuscript. Zhang XF, Yang MM, Guo YC, Yang HX, Zhang M, Li C, Wei LX and Bi HT contributed to the interpretation of data and critically revised the manuscript. All authors have approved the final version of the manuscript.

## Competing interests

The authors declare no conflicts of interest.

## Acknowledgments

This work was supported by the Key project of Chinese Academy of Sciences (Grant No. ZDRW-ZS-2020-2), Innovation Platform Program of Qinghai Province (2021-ZJ-T02), Key Laboratory Project of Qinghai Province (2022-ZJ-Y05), the Natural Science Foundation of China (Grant No. 82171863), and China Postdoctoral Science Foundation funded project (2021M701642).

## Peer review information

Traditional Medicine Research thanks Hong Li and other anonymous reviewers for their contribution to the peer review of this paper.

## Abbreviations

PBC, primary biliary cholangitis; OCA, obeticholic acid; SMF, *Swertia mussoyii* Franch.; EMT, epithelial-mesenchymal transition; HIBEC, human intrahepatic biliary epithelial cells; PCA, principal component analysis; OPLS-DA, orthogonal partial least squares-discriminant analysis; DEG, differentially expressed genes; OMIM, Online Mendelian Inheritance in Man.

## Citation

Zhang XF, Yang MM, Guo YC, et al. Study on the effect and mechanism of *Swertia mussoyii* Franch. in the treatment of primary biliary cholangitis based on bioinformatics and in vitro experiments. *Tradit Med Res.* 2024;9(3):16. doi: 10.53388/TMR20230915004.

Executive editor: Xi-Yue Liu.

Received: 15 September 2023; Accepted: 07 December 2023;

Available online: 11 December 2023.

© 2024 By Author(s). Published by TMR Publishing Group Limited. This is an open access article under the CC-BY license. (<https://creativecommons.org/licenses/by/4.0/>)

## Abstract

**Background:** Primary biliary cholangitis (PBC) is a chronic biliary autoimmune liver disease characterized by intrahepatic cholestasis. *Swertia mussoyii* Franch. (SMF) is a Tibetan medicine with hepatoprotective and anti-inflammatory activities. In this study, the therapeutic effect and potential mechanisms of SMF on PBC were investigated by bioinformatics analysis and in vitro experimental validation, with the aim of promoting the progress of SMF and PBC research. **Methods:** We first explored the therapeutic effects and key targets of SMF on PBC using a network pharmacology approach, further screened the core targets using the GSE79850 dataset, and finally validated the results using molecular docking techniques and in vitro experiments. **Results:** By bioinformatics analysis, we identified core targets of SMF for PBC treatment (STAT3, JAK2, TNF- $\alpha$ , and IL-1 $\beta$ ) and important signaling pathways: JAK-STAT, TNF, and PI3K-AKT. The molecular docking results showed that the significant components of SMF had good binding properties to the core targets. In vitro experiments showed that SMF extracts improved the extent of epithelial-mesenchymal transition in human intrahepatic biliary epithelial cells and had a significant reversal effect on epithelial-mesenchymal transition process markers and potential targets in PBC. **Conclusion:** SMF may exert its therapeutic effects on PBC by acting on important targets such as STAT3, JAK2, TNF- $\alpha$ , IL-1 $\beta$ , Vimentin, and E-cadherin and the pathways in which they are involved.

**Keywords:** *Swertia mussoyii* Franch.; primary biliary cholangitis; bioinformatics; in vitro experiments

**Highlights**

*Swertia mussotii* Franch. showed significant inhibition of the epithelial mesenchymal transition process in the development and progression of primary biliary cholangitis. *Swertia mussotii* Franch. may play a therapeutic role for primary biliary cholangitis by acting on STAT3, JAK2, TNF- $\alpha$ , IL-1 $\beta$ , Vimentin and E-cadherin.

**Medical history of objective**

As a herb of *Gentianaceae* family, *Swertia mussotii* Franch. is widely used in Tibetan pharmacology, mainly in Qinghai, Tibet and Sichuan, etc. It is considered to have good hepatoprotective and choleric effects and has been used for long time in the treatment of jaundice. Its unique herbal composition is documented in classic Tibetan medicine texts, such as the *Four Medical Classics* (8th–12th century) and the *Jingzhu Materia Medica* (1840 C.E.), which mention the medicinal value of *swertia*. This signifies the prominent role of *Swertia mussotii* Franch. in Tibetan medicinal traditions, being regarded by the local population as a precious natural herbal remedy.

**Introduction**

Primary biliary cholangitis (PBC), also known as primary biliary cirrhosis, is a chronic biliary autoimmune liver disease characterized by intrahepatic cholestasis and nonsuppurative inflammatory destruction. PBC leads to extensive hepatic duct destruction and the presence of anti-mitochondrial antibodies, which eventually progress to liver fibrosis, cirrhosis, and liver failure [1]. The main population of PBC is middle-aged women, and the pathogenesis is complex and multifactorial, with a combination of genetic and environmental factors determining the onset and persistence of the disease [2–4]. Several publications have reported that PBC is closely associated with immune abnormalities [5]. The involvement of multiple immune cells, such as CD4<sup>+</sup> T, CD8<sup>+</sup> T, and B cells, has been detected in patients with PBC, while other immune cells, such as dendritic cells, natural killer cells, monocytes, and macrophages, are also important [6]. Ursodeoxycholic acid is the only first-line drug for the treatment of this disease, and related studies claim that approximately 40% of patients respond poorly [7, 8]. Although obeticholic acid (OCA) is also often used in the treatment of PBC, it can lead to severe liver damage [9]. Therefore, exploration of the pathogenesis of PBC and the development of new therapeutic agents are necessary.

Epithelial mesenchymal transition is a biological process in which epithelial cells with polarity lose their epithelial characteristics and gradually transform into mesenchymal cells with migratory and invasive abilities. Studies have shown that EMT of bile duct epithelial cells is an important process of liver fibrosis in PBC and that bile duct cells undergo EMT when stimulated by cytokines such as TGF- $\beta$ , which may promote the development of liver fibrosis in cholestatic liver disease [10]. Several studies have suggested that EMT is a key pathogenic process and initiating event in PBC and that prevention of EMT can control or even reverse liver fibrosis [11–13]. Thus, inhibiting the EMT process in intrahepatic bile duct epithelial cells would reduce or reverse liver fibrosis, which offers a greater possibility for the treatment of PBC.

Traditional Chinese medicine is mainly composed of herbs and plants and is widely used to treat various diseases [14]. Various studies have shown that Chinese medicine is highly efficacious and has few side effects [15]. Tibetan medicine is an important part of traditional Chinese medicine. As an ethnic medicine, Tibetan medicine is the treasure of the Chinese nation. *Swertia mussotii* Franch. (SMF) is an annual herb of the family *Gentianaceae*, genus *Swertia*. It is mainly distributed in Qinghai, Tibet, Yunnan, and other regions of China. As a traditional Tibetan medicine, it has been used for thousands of years on the Qinghai-Tibetan Plateau to treat liver diseases [16, 17].

Recently, significant progress has been made in the study of the chemical composition of SMF. Studies have shown that SMF is rich in bioactive compounds such as flavonoids, xanthenes, iridoids, and alkaloids [18, 19]. Modern pharmacological studies have shown that SMF exhibits a variety of positive pharmacological activities, such as hepatoprotective effects, anti-inflammatory activity, and antibacterial, antitumor, hypoglycemic, and skin care effects. Yun et al. showed that SMF treatment improved alanine aminotransferase, aspartate aminotransferase, and total bilirubin levels in rats with acute liver injury [17]. Chai et al. showed that oral administration of components from SMF reduced liver injury, inflammation, and biliary blockage in rats with bile duct ligation [20]. As is well-established, within traditional medicine, PBC is categorized under “jaundice” (This disorder, known in modern medicine as hyperbilirubinemia, is a yellow staining of the skin or organs caused by an increase and buildup of bilirubin in the body), and Yin Chen serves as a pivotal remedy for jaundice in the realm of traditional Chinese medicine [21, 22]. Interestingly, SMF is also known as “Zang Yin Chen”, documented in the *Four Medical Classics* and the *Jingzhu Materia Medica*, also has been reported to be a traditional herbal medicine for jaundice [23, 24]. Therefore, for these reasons, the present study was conducted on SMF for the treatment of PBC.

With the development of bioinformatics, network pharmacology is being widely and increasingly used to study the mechanisms of herbal medicines. Network pharmacology is based on the “multicomponent, multitarget” theory, which coincides with the characteristics of traditional Chinese medicine. Network pharmacology has been widely used to screen for active ingredients in traditional Chinese medicine, to determine new uses for existing drugs, and to explore potential targets. On this basis, the joint study of network pharmacology, gene expression profile data from the GEO database, and molecular docking techniques has become a mainstream type of research. In this study, we first explored the potential mechanisms and key targets of the active ingredients in SMF for the treatment of PBC using a network pharmacology approach. We further screened the core targets using the gene expression profile data from the GEO database and then verified the binding of the significant components to the core targets using molecular docking techniques. Finally, we verified the inhibitory effect of SMF extract on human intrahepatic biliary epithelial cells (HIBEC)-EMT by in vitro experiments. This paper provides new ideas and potential methods for the study and treatment of PBC and promotes SMF as a potential treatment for PBC.

**Methods****Network pharmacology**

**Acquisition of compounds in SMF.** We obtained the chemical composition through literature research [25]. We prepared the structures of these compounds using Chemdraw, placed them in the lowest energy state using Chem3D’s “Minimize Energy” function, and exported them to mol2 and smi formats for subsequent analysis [26].

**Screening of active ingredients.** SwissADME is a platform that allows the prediction of ADME parameters, pharmacokinetic properties, drug-like properties, and medicinal chemistry friendliness of small molecules to support drug discovery [27]. Gastrointestinal absorption was the criterion used for oral bioavailability in the SwissADME platform; we also used Lipinski’s drug-like properties in our screening. Lipinski’s rule requires a molecular weight  $\leq$  500 g/mol, lipid-water partition coefficient (MLOGP)  $\leq$  4.15, number of H-bond acceptors (N or O)  $\leq$  10, and number of H-bond donors (NH or OH)  $\leq$  5. We used the result that ; Gastrointestinal absorption is high for the compound to be well absorbed and to comply with Lipinski’s rule in the prediction of drug-likeness (“Lipinski” marked as “Yes; 0 violation”). If these two conditions were met, the compound could be screened as a potential active compound. We uploaded the smi format of the 138 chemical components to the SwissADME platform and screened them according to the information obtained from the predictions and following the criteria described previously. Finally, we used the PAINS Remover platform to re-screen the

obtained compounds (obtained by screening on the SwissADME platform) to remove false-positive drugs and obtain the active ingredients [28].

**Target prediction of active ingredients.** PharmMapper and SwissTargetPrediction are two platforms that have been widely used for predicting compound targets [29–32]. PharmMapper focuses on known small molecule compounds to identify their possible targets using data from the TargetBank, DrugBank, BindingDB, and PDTD databases. SwissTargetPrediction uses similarity to the 2D and 3D structures of known compounds to predict the targets of compounds, along with known compound-target interactions from the ChEMBL database. We uploaded the active ingredients to the PharmMapper platform in the mol2 format and to the SwissTargetPrediction platform in the smi format to obtain the potential targets. In the SwissTargetPrediction platform results, we excluded targets with a probability\* of 0. We performed an ID transformation of the results obtained from the PharmMapper platform through the UniProt database to obtain the corresponding target names. Finally, we merged the results from both platforms.

**Target collection for PBC disease and identification of common targets with SMF.** GeneCards is an integrated database that automatically retrieves and integrates data from 125 databases [33]. Online Mendelian Inheritance in Man (OMIM) is a comprehensive, authoritative database for the study of human phenotypic and genotypic relationships, with information on all known Mendelian diseases [34]. We searched the GeneCards and OMIM databases with the keyword “Primary biliary cholangitis” to obtain disease-related targets and combined the results of the two databases to obtain PBC targets. Next, we took the intersection of the targets of the active ingredients and the targets of PBC for subsequent analysis. The study was conducted in accordance with the Declaration of Helsinki (as revised in 2013).

**PPI and enrichment analysis.** The STRING database is mainly used to predict protein interactions [35]. We uploaded the intersecting targets to the STRING database with the following parameters: homo sapiens, hide the disconnected nodes, and high confidence to obtain information on the PPI network. In addition, we performed the KEGG pathway enrichment analysis and GO enrichment analysis. KEGG pathway enrichment analysis is mainly used to observe the biological pathways in which targets may be involved, while GO enrichment analysis mainly includes biological processes, molecular functions, and cellular components. We uploaded the common targets of PBC and SMF to the Metascape platform for enrichment analysis using  $P < 0.01$  and selected the top 20 for each for mapping [36].

**Network construction.** Cytoscape is an open-source software focused on network visualization and analysis [37]. We collated information related to the drug-active ingredient, active ingredient-target, PPI, and protein-pathway interactions and constructed the network using Cytoscape software (drug, active ingredients, targets, and pathways are represented by nodes, and interactions are represented by edge connections). After analyzing the network, the targets with the top 10-degree values were used as key targets, and the components with the top 5-degree values were used as significant components for subsequent studies.

#### GEO data analysis

**Acquisition of PBC expression profile data.** GEO is a gene expression database created and maintained by the National Center for Biotechnology Information. It contains high-throughput gene expression data submitted by research institutions worldwide. We obtained the GSE79850 data through the GEO platform [38]. This dataset consists of high- (n = 9) and low-risk (n = 7) patient material along with nondisease control livers (n = 8), which we divided into two groups (PBC group (n = 16) and control group (n = 8)) for follow-up studies.

**Principal component analysis (PCA) and orthogonal partial least squares-discriminant analysis (OPLS-DA).** PCA is a traditional statistical method introduced by the field of machine learning that is an unsupervised learning algorithm mainly used for data

dimensionality reduction. OPLS-DA is a supervised statistical method for discriminant analysis. Partial least squares regression is used to model the relationship between the amount of material expression and the sample category. We performed PCA and OPLS-DA on the samples included in GSE79850 to observe the variability between the PBC group and the control group.

**Differential expression analysis.** GEO2R is a tool used for further differential analysis of the expression profile microarrays in the GEO database. Using this tool, two or more groups of samples in the GEO series can be compared to obtain differentially expressed genes (DEGs) [39]. We performed differential expression analysis between the PBC and control groups using the GEO2R tool, screened DEGs using  $|\log_2\text{-fold change}| \geq 1$  and  $P < 0.05$ , and generated volcano plots via an online platform (<https://www.bioinformatics.com.cn>).

**Screening of Important DEGs.** We identified the intersection of DEGs in GSE79850 with the key targets obtained from network pharmacology to further screen for core targets. We then extracted their expression in the PBC and control groups through an unpaired sample *t*-test using GraphPad Prism 9.0.

**Immune correlation analysis.** Studies have shown that the immune system is disordered in patients with PBC. Therefore, we performed an immune correlation analysis. We first used the CIBERSORT algorithm to visualize the proportions of 22 immune cell types in 24 samples using the R package. Furthermore, correlation analysis was performed between the core targets obtained by the above process and various immune cell proportions to observe their relationships.

#### Molecular docking

AutoDock Vina is an open-source molecular docking software that presents results in the form of binding energy [40]. We used the core targets as receptors, and the significant components with the top 5-degree values were used as ligands for molecular docking using AutoDock Vina. During the docking process, we constructed boxes centered on the target and completely wrapped the protein to explore possible binding sites for small molecules and to seek the best binding mode with the lowest binding energy while the rest of the parameters were set by default. The final docking results were visualized with PyMOL software.

#### In vitro experimental validation

**Material and Reagents.** HIBEC and complete medium (ZQ-1315) were purchased from Zhong Qiao Xin Zhou Biotechnology Co. Ltd. (Shanghai, China); OCA (Batch number: A012321) was purchased from Wuhan XINSHENSHI Chemical Technology Co., Ltd. (Wuhan, China); ELISA kits for TNF- $\alpha$  (Batch number: 09/2022) and IL-1 $\beta$  (Batch number: 09/2022) were purchased from Jianglai Biotechnology Co., Ltd. (Shanghai, China); ELISA kits for STAT3 (Batch number: 20230414XT), JAK2 (Batch number: 20230414XP), Vimentin (Batch number: 20230414XN) and E-cadherin (Batch number: 20230414XI) were purchased from Jingmei Biotechnology Co., Ltd. (Jiangsu, China).

The SMF was collected from the Tongtian River basin in Chengduo County, Yushu Prefecture, Qinghai Province, China, and was identified by Professor Yubi Zhou from the Northwest Institute of Plateau Biology, Chinese Academy of Sciences, with sample number NWIPB-201909. Preparation of SMF extract: The extract was extracted twice with 75% ethanol at 60 °C under hot reflux for 60 min each time, separated by a macroporous resin column DM301 and eluted with 20% ethanol.

**Cell culture.** HIBECs were cultured in complete medium ZQ-1315 containing 2% fetal bovine serum, 1% epithelial growth factor, and 1% penicillin–streptomycin at 37 °C and 5% CO<sub>2</sub>.

**Effect of cytotoxic viability test and SMF extract on the cellular viability of HIBEC-EMT.** HIBEC cells were seeded in 96-well plates at a density of 104 and cultured for 24 h. After that, the experiments were divided into 4 groups, including the control group, SMF-L group (low dose: 600  $\mu\text{g}/\text{mL}$ ), SMF-M group (medium dose: 800  $\mu\text{g}/\text{mL}$ ), and SMF-H group (high dose: 1000  $\mu\text{g}/\text{mL}$ ). The original medium was discarded, and the normal medium was added to the control group,

while the SMF-L, SMF-M, and SMF-H groups were added to the medium containing the corresponding SMF extract concentrations. Twenty-four hours later, MTT assays were performed to observe cytotoxicity.

HIBEC cells were seeded in 96-well plates at a density of 104 and cultured for 24 h. After that, the experiments were divided into 6 groups, including the control, model, OCA (41.6 ng/mL), SMF-L, SMF-M, and SMF-H groups [41]. The original culture medium was discarded, and a normal culture medium was added to the control group, while a medium containing 100 ng/mL TGF- $\beta$ 1 was added to the rest of the groups. Twelve hours later, the culture medium was discarded, and the normal culture medium was added to the control and model groups. Medium containing OCA was added to the OCA group, and medium containing the corresponding concentration of SMF extract was added to the low-, medium-, and high-dose groups. After 24 h, MTT experiments were performed to detect the viability of the cells.

**Mechanistic study of SMF extract against HIBEC-EMT.** HIBEC cells were grown in 6-well plates at 350,000/3 mL and cultured for 24 h. After that, the experiment was divided into 6 groups, including the control group, model group, OCA group, SMF-L group, SMF-M group, and SMF-H group. The model was constructed and administered according to the method described above. Twenty-four hours after drug administration, the cells and supernatants in the 6-well plates were collected separately, and the concentrations of TNF- $\alpha$  and IL-1 $\beta$  in the supernatants and the concentrations of intracellular proteins (JAK2, STAT3, Vimentin, and E-cadherin) were detected according to the ELISA kit instructions.

**Statistical analysis.** All statistical analyses were performed using SPSS 26.0 software, and the results are presented as the mean  $\pm$

standard error of mean. Comparisons of differences between groups were performed by one-way ANOVA and plotted using GraphPad Prism 9.0.

## Results

### Network pharmacology

**Compound collection and screening of active ingredients.** We obtained a total of 138 chemical components; their mol2 and smi formats were obtained using Chem Office software. After uploading these 138 compounds to SwissADME, a total of 43 ingredients were obtained based on the criteria described in the Methods section. Finally, through The PAINS Remover platform, we obtained 39 active ingredients. The specific information is presented in [Supplementary Table S1](#), and their "SMILES" are provided in [Supplementary Table S2](#). **Common targets of the active ingredients and PBC.** As previously described, we uploaded the 39 active ingredients to the PharmMapper and SwissTargetPrediction platforms to obtain potential targets. After collation, a total of 2,779 targets were obtained for the active ingredient targets. After searching PBC targets in GeneCards and OMIM, 1,522 targets were obtained following the merging. We identified the intersection between the targets of the active ingredients and the targets of disease to obtain a total of 203 common targets ([Figure 1](#)).

**Enrichment analysis results.** We uploaded 203 common targets to the Metascape platform for KEGG pathway and GO enrichment analyses, which resulted in 201 pathways, 1,915 GO biological processes, 98 GO cellular components, and 173 GO molecular functions. We selected the top 20 in each project for graphing; these are shown in [Figure 2](#). KEGG pathway enrichment analysis identified

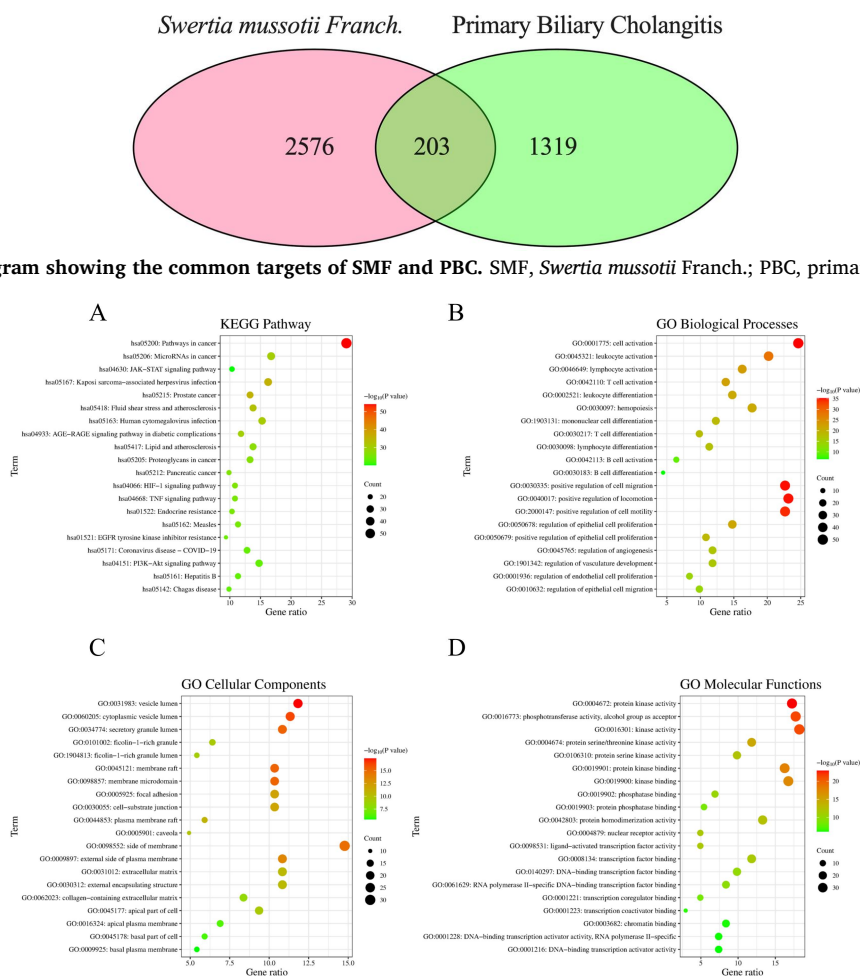


**Figure 2 Enrichment analysis results.** (A) KEGG pathway enrichment analysis; (B) GO biological processes; (C) GO cellular components; (D) GO molecular functions.

three important pathways: the JAK-STAT, TNF, and PI3K-AKT signaling pathways. The active ingredients in SMF may act on these pathways and thus play a role in the treatment of PBC. GO enrichment analysis showed that biological processes is mainly involved in inflammatory and immune-related processes, cellular components results showed that these targets act mainly at the plasma membrane site, and molecular functions results showed that these targets may be associated with kinase.

**Network construction of the drug-component-target (PPI)-pathway.** We collated the information related to drug-active ingredients, active ingredients-common targets, PPI, and targets-pathways and mapped the network in Cytoscape (Figure 3). This network contained a total of 263 nodes (drug: 1; ingredients: 39;

targets: 203; pathways: 20) and 2,629 edges (drug-ingredients: 39; ingredients-targets: 942; PPI: 1112; targets-pathways: 536). In this network, key targets with top 10-degree values and significant components with top 5-degree values were used for subsequent analysis.

#### GEO data analysis

**Multivariate statistical analysis and differential expression analysis.** We performed PCA and OPLS-DA on 24 samples. The results showed that the two groups were clearly separated and showed a significant difference between the two groups (Figure 4A, 4B). In addition, GSE79850 was differentially analyzed using the GEO2R tool

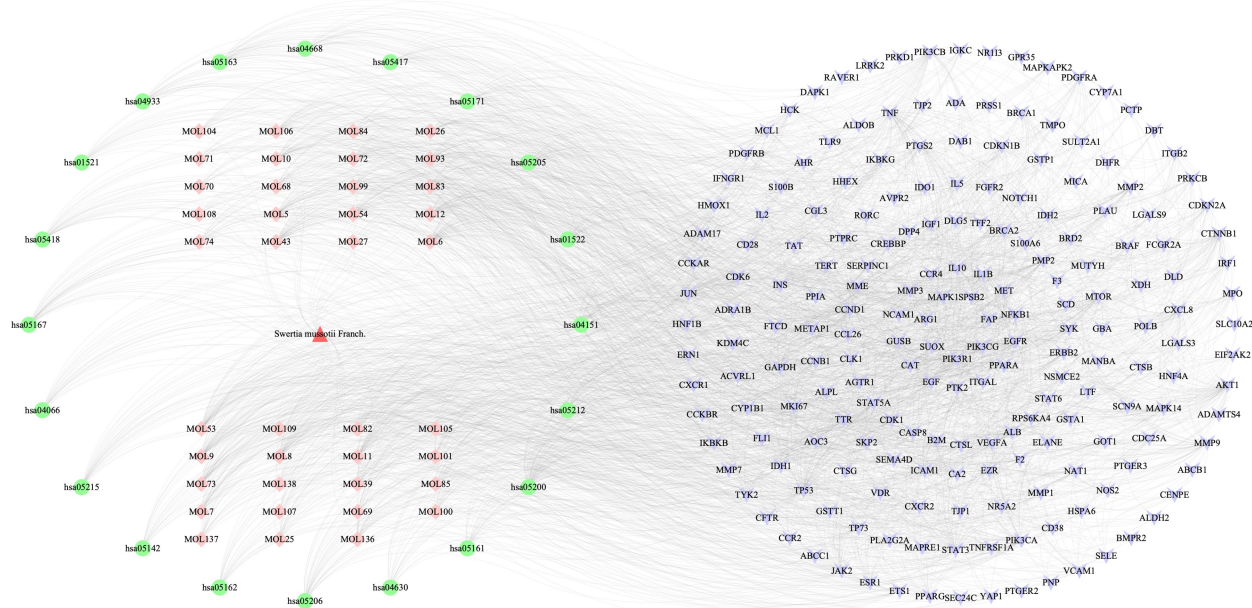


**Figure 3 Drug-active ingredient-target (PPI)-pathway network.** Triangles represent the drug, diamonds represent the active ingredients, V represents the target, and circles represent the pathways.

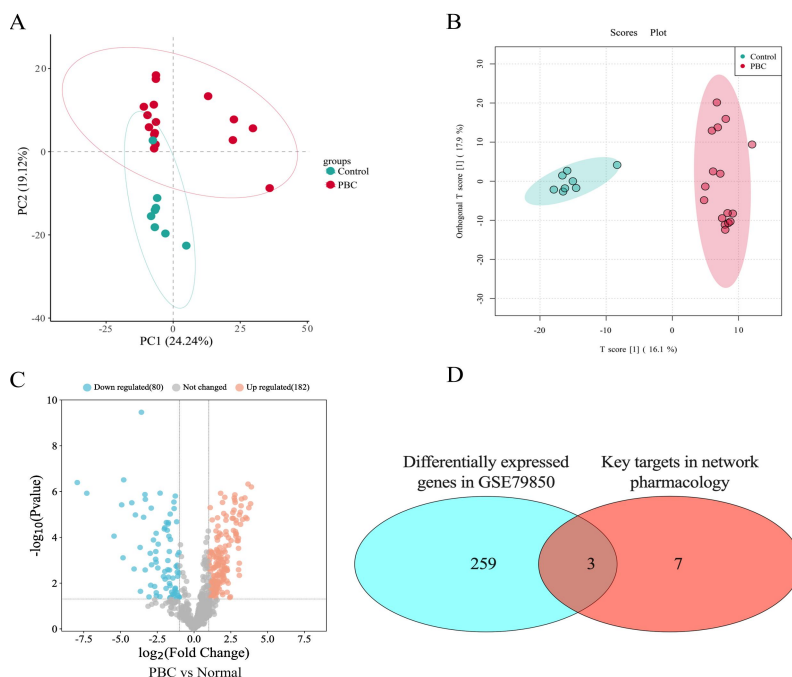


**Figure 4 Results of multivariate statistical analysis and differential expression analysis of GSE79850.** (A) Results of PCA; (B) Results of OPLS-DA; (C) Results of the GSE79850 differential expression analysis; (D) Venn diagram of the intersection of DEGs from GSE79850 with key targets from network pharmacology. PCA, principal component analysis; OPLS-DA, orthogonal partial least squares-discriminant analysis.

(Figure 4C). A total of 262 genes were DEGs, of which 182 genes were up-regulated, and 80 genes were down-regulated. Then, we obtained three core targets (STAT3, TNF- $\alpha$ , and IL-1 $\beta$ ) by taking the intersection of the top 10 key targets obtained with network pharmacology and the 262 DEGs obtained from GSE79850 (Figure 4D). These three core targets are involved in three pathways obtained from the KEGG pathway enrichment analysis: JAK-STAT, TNF, and PI3K-AKT signaling pathways. Since JAK2 is a key node of the JAK-STAT pathway, we also included JAK2 as a core target to be investigated in subsequent studies.

**Immune correlation analysis.** We visualized the proportion of 22 immune cell species in 24 samples using the R package and the CIBERSORT algorithm (Figure 5A). Comparisons between groups were also performed (Figure 5B), which showed that compared to the control group, the proportions of B cells naive, Monocytes, Mast cells resting, and Neutrophils were significantly reduced, while the proportions of T cells CD4 memory resting and Macrophages M1 significantly increased in the PBC group. To further explore the

correlation between the core targets and the proportion of various immune cell types, we performed a correlation analysis (Figure 5C). The results showed a good correlation between the expression of these core targets and the proportion of various immune cell types.

#### Molecular docking

We used these core targets as receptors and the significant components that ranked in the top five in terms of degree value as ligands for molecular docking. The structure of the receptor was obtained from the PDB database, the details of which are provided in Supplementary Table S3. Using AutoDock Vina, the results showed that they all had good binding properties (Table 1 and Figure 6A). Finally, we selected the results with the lowest binding energy of each protein to small molecules in molecular docking and visualized them using PyMOL, as shown in Figure 6B–6F).

#### In vitro cellular assay results

**Cytotoxic activity assay and the effect of SMF on fibrotic HIBECs.**

**Table 1 Molecular docking results**

Degree	Compound	Target	UniProt ID	PDB ID	Binding energy (kcal/mol)	Binding sites	Numbers of hydrogen bonds
49	MOL 53	STAT3	P40763	6TLC	-7.0	LYS-363, TRY-360, LYS-282	4
		TNF- $\alpha$	P01375	7KPB	-8.3	ASN-92, THR-94, GLN-82, CYS-96	5
		IL-1 $\beta$	P01584	9ILB	-7.2	SER-43, TYR-68	4
		JAK2	O60674	7RN6	-8.0	GLU-898	1
46	MOL 6	STAT3	P40763	6TLC	-6.3	LYS-370, ASP-369	3
		TNF- $\alpha$	P01375	7KPB	-7.1	SER-86, ARG-68	2
		IL-1 $\beta$	P01584	9ILB	-6.6	SER-43, TYR-68	3
		JAK2	O60674	7RN6	-7.5	ASP-994	1
45	MOL 9	STAT3	P40763	6TLC	-7.4	GLN-361, GLU-357	3
		TNF- $\alpha$	P01375	7KPB	-7.3	ARG-68, ARG-82, ASN-34	4
		IL-1 $\beta$	P01584	9ILB	-6.5	ASN-7, SER-43, TYR-68	4
		JAK2	O60674	7RN6	-8.3	ASP-994	1
42	MOL 43	STAT3	P40763	6TLC	-6.4	GLN-326, ALA-250, SER-514, ASP-334	4
		TNF- $\alpha$	P01375	7KPB	-6.9	SER-30	1
		IL-1 $\beta$	P01584	9ILB	-6.5	ASN-7, SER-53, PRO-87, TYR-68	5
		JAK2	O60674	7RN6	-8.1	LYS-882, PHE-995, LEU-932	4
42	MOL 8	STAT3	P40763	6TLC	-7.2	GLN-361	2
		TNF- $\alpha$	P01375	7KPB	-7.5	LYS-75, ARG-77, CYS-96	3
		IL-1 $\beta$	P01584	9ILB	-6.5	ASN-7, SER-43, TYR-68	4
		JAK2	O60674	7RN6	-8.3	ARG-975, ILE-973	2

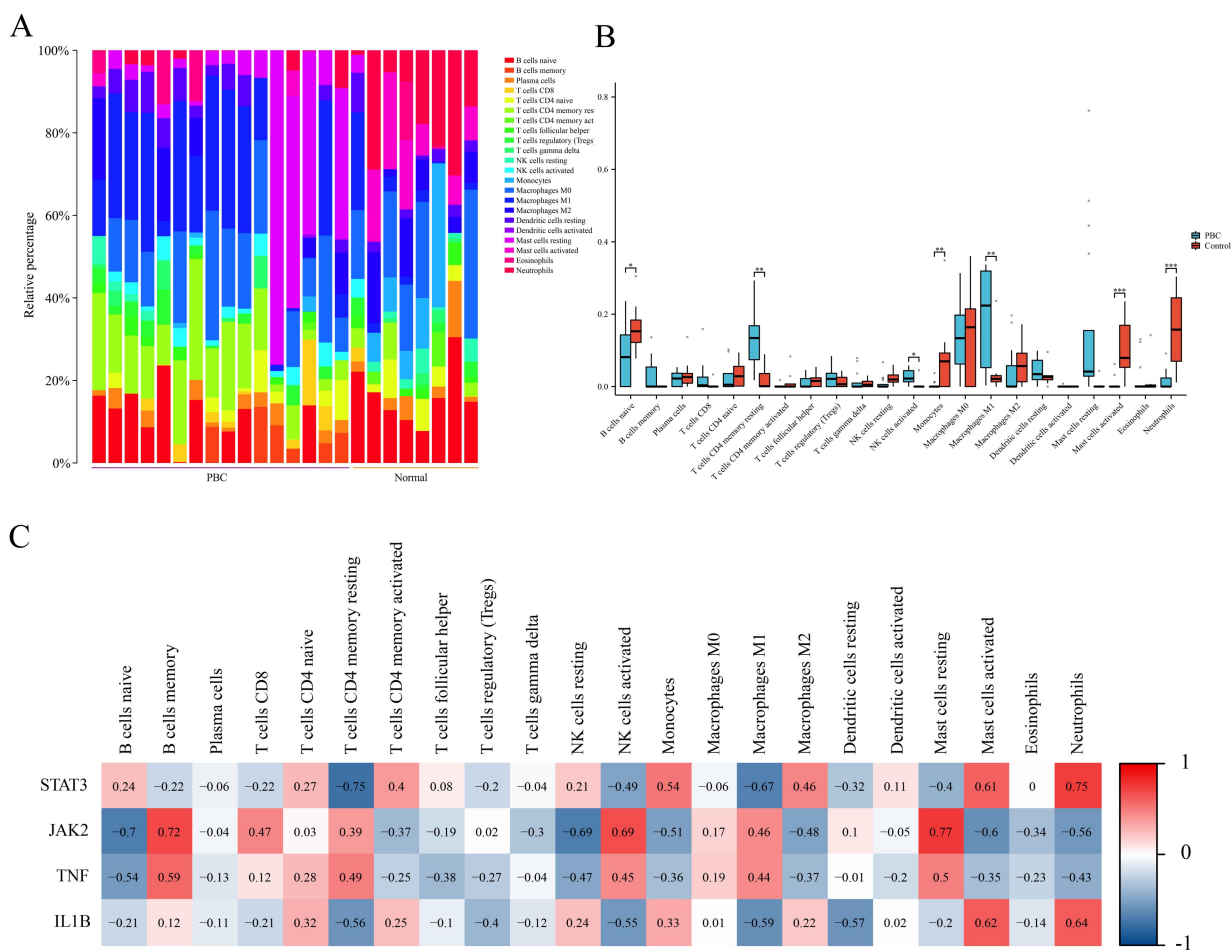


**Figure 5 Results of the immune correlation analysis.** (A) Visualization of the proportions of 22 immune cell types in 24 samples. (B) Comparative results of intergroup analysis of 22 immune cell ratios; (C) Correlation between core targets and the proportion of 22 immune cell types. Compared with the control group, \* $P < 0.05$ , \*\* $P < 0.01$ , \*\*\* $P < 0.001$ .

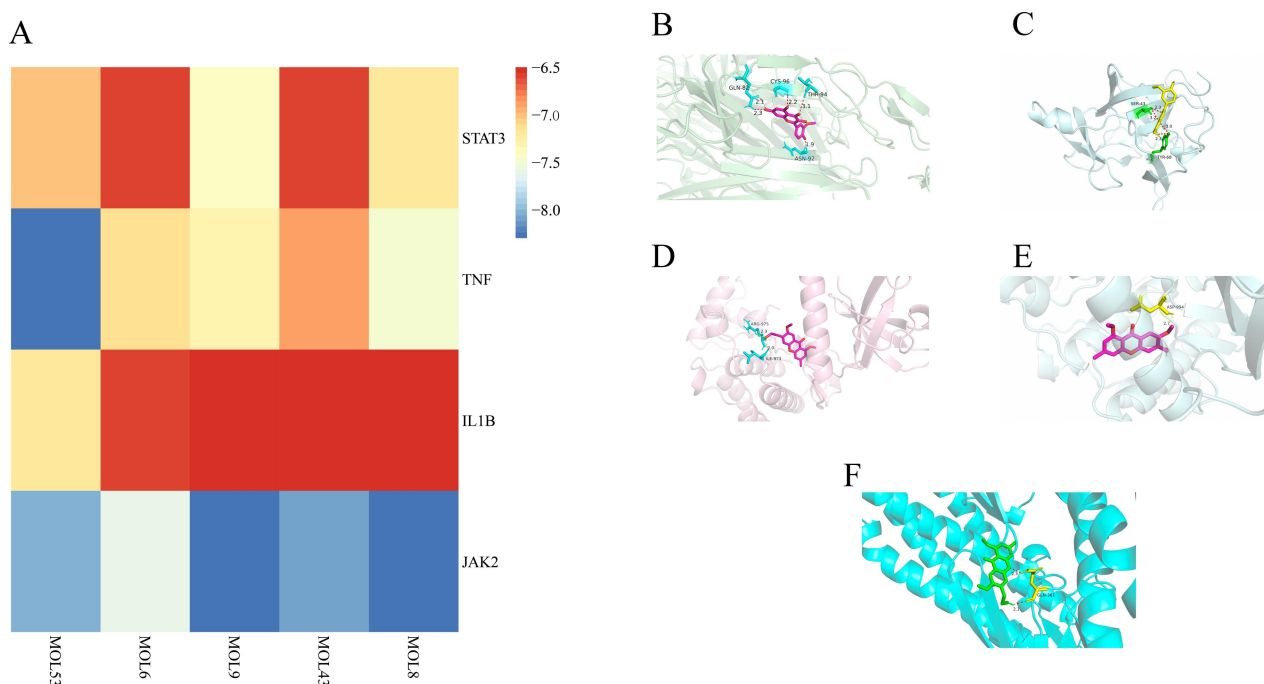


**Figure 6 Results of molecular docking.** (A) Molecular docking binding energy heatmap. (B) Visualization of TNF- $\alpha$  and MOL 53 molecular docking result; (C) Visualization of IL-1 $\beta$  and MOL 53 molecular docking result; (D) Visualization of JAK2 and MOL 8 molecular docking result; (E) Visualization of JAK2 and MOL 9 molecular docking result; (F) Visualization of STAT3 and MOL 8 molecular docking results.

The results of the cytotoxic activity assay are shown in Figure 7A, which showed significant inhibition of HIBEC cellular viability at a high dose of 1,000 µg/mL. We induced EMT in HIBECs by TGF-β1 and further explored the effect of SMF extract on HIBEC-EMT by administering different concentrations of SMF. We found that OCA, SMF-L, SMF-M, and SMF-H all significantly improved the viability of HIBEC-EMT cells, as shown in Figures 7B, 7C.

**Study on the mechanism of reversal of the effect of SMF on HIBEC-EMT.** We collected intracellular proteins as described in the ELISA kit for HIBEC-EMT markers (Vimentin and E-cadherin), STAT3, and JAK2, and the results are shown in Figures 8A, 8B, 8E, 8F. The levels of E-cadherin and STAT3 were significantly decreased in the model group, and the levels of Vimentin and JAK2 were significantly increased, and this phenomenon was reversed by treatment with both

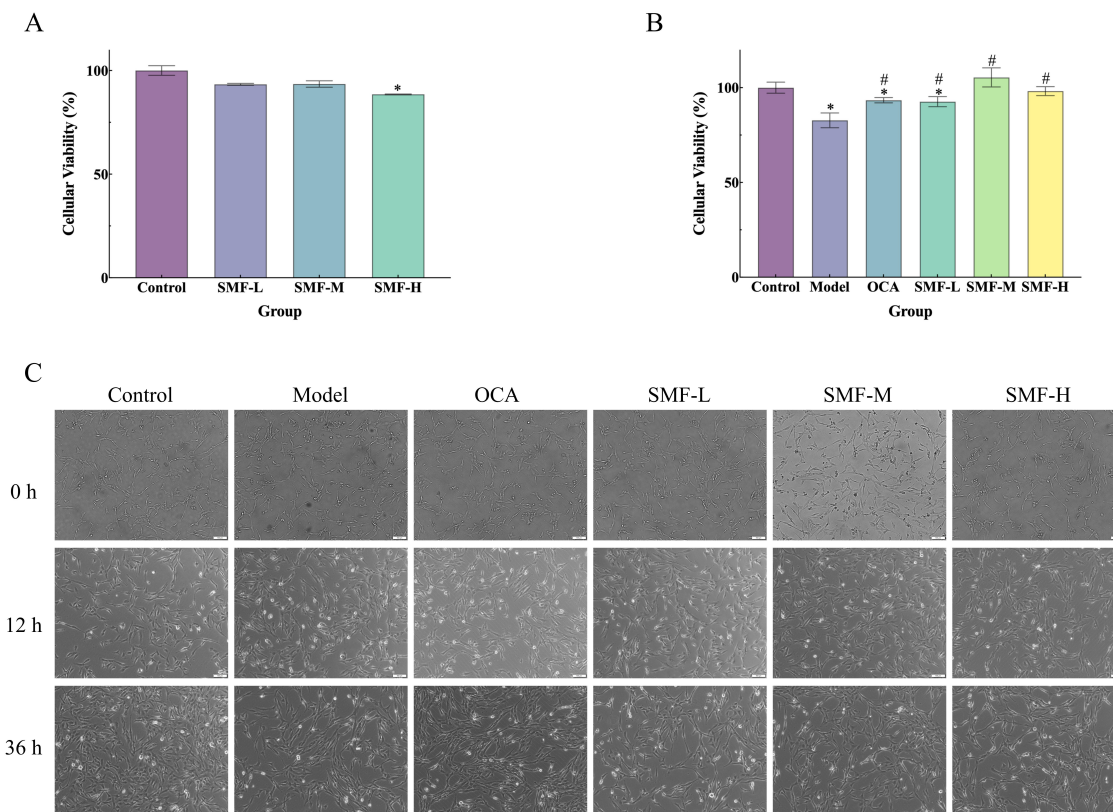


**Figure 7** Effect of SMF on the viability of HIBECs and HIBEC-EMT. (A) SMF on normal HIBEC cytotoxic viability test; (B) SMF on HIBEC-EMT cell viability test; (C) Cellular status of HIBEC before model construction, after modeling, and after drug treatment. Compared with the control group,  $P < 0.05$ ; compared with the model group,  $\#P < 0.05$ . SMF, *Swertia mussotii* Franch.; EMT, epithelial-mesenchymal transition; HIBEC, human intrahepatic biliary epithelial cells.

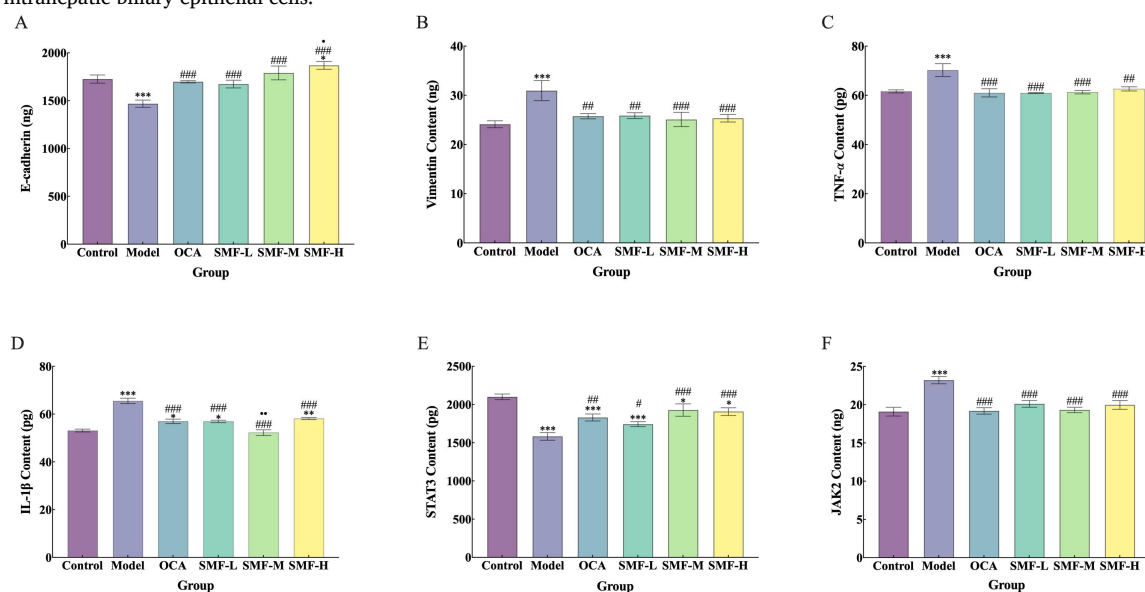


**Figure 8** Results of the ELISA kit for protein levels. (A) Results of E-cadherin level measurements; (B) Results of Vimentin level measurements; (C) Results of TNF-α level measurements; (D) Results of IL-1β level measurements; (E) Results of STAT3 level measurements; (F) Results of JAK2 level measurements. Compared with the control group,  $*P < 0.05$ ,  $**P < 0.01$ ,  $***P < 0.001$ ; compared with the model group,  $\#P < 0.05$ ,  $\#\#P < 0.01$ ,  $\#\#\#P < 0.001$ ; compared with the OCA group,  $\textcircled{P} < 0.05$ ,  $\textcircled{P} < 0.01$ ,  $\textcircled{P} < 0.001$ . OCA, obeticholic acid.

OCA and SMF extracts. We measured TNF- $\alpha$  and IL-1 $\beta$  levels by collecting cell supernatants as described in the Methods, and the results are shown in Figures 8C, 8D; both indicators were significantly elevated in the model group, while TNF- $\alpha$  and IL-1 $\beta$  levels were significantly reduced in the OCA, SMF-L, SMF-M, and SMF-H groups. The above results indicate that SMF has a therapeutic effect on HIBEC-EMT.

### Discussion

We investigated the treatment of PBC by SMF through deep mining of network pharmacology and GEO datasets. Finally, we obtained core targets for SMF treatment of PBC, and we validated these results by in vitro experiments with consistent results.

GO enrichment analysis revealed that SMF acting on the targets of PBC is mainly involved in the immune and inflammatory responses. The development and progression of PBC is accompanied by severe immune disorders and inflammatory responses, and current treatment is mainly achieved by modulating the immune system and reducing the inflammatory response [42]. KEGG pathway enrichment analysis showed that SMF may exert therapeutic effects mainly through regulation of the JAK-STAT, TNF, and PI3K-AKT signaling pathways. The JAK-STAT pathway is a major signaling mechanism for a variety of cytokines and growth factors. Activation of JAK stimulates cell proliferation, differentiation, cell migration, and apoptosis. The substrate of JAK is STAT, which is phosphorylated by JAK and then dimerizes before crossing the nuclear membrane to regulate the expression of related genes. The results of an international genome-wide meta-analysis highlighted the importance of JAK-STAT signaling and TNF signaling in the pathogenesis of PBC [43]. An overview of the pathogenesis of PBC highlighted the HLA-II-like regions and genes associated with IL12-JAK/STAT signaling, as well as the important role of the NF- $\kappa$ B and TNF signaling pathways in PBC [44]. PI3K-AKT is a RTK-mediated signaling pathway that is associated with phosphatidylinositol. PI3K-AKT signaling begins with the activation of RTK and cytokine receptors. The importance of PI3K-AKT in hepatobiliary diseases has been highlighted in several studies [45, 46]. In addition, studies have shown that related plants or active ingredients of the genus *Swertia* may exert good therapeutic effects on liver diseases through the PI3K-AKT signaling pathway [47, 48]. In summary, the JAK-STAT, TNF, and PI3K-AKT signaling pathways may be potential mechanisms of SMF in the treatment of PBC. However, this conclusion needs to be validated by further studies.

We obtained the GSE79850 dataset through the GEO platform and further performed difference analysis using the GEO2R tool to obtain 262 DEGs. The PCA and OPLS-DA results showed that the PBC group and the control group could be clearly divided into two groups. Then, we took the intersection of these 262 DEGs with the 10 key targets obtained via network pharmacology and identified core targets. STAT3 is a member of the STAT family. In response to cytokines and growth factors, STAT family members are phosphorylated by receptor-associated kinases and then form homodimers or heterodimers that are translocated to the nucleus, where they act as transcriptional activators. Studies have shown that inflammatory factor levels are abnormally significant in patients with PBC. In addition, STAT3 phosphorylation induces ER $\alpha$ -mediated expression of proinflammatory cytokines [49]. TNF- $\alpha$  and IL-1 $\beta$  are important inflammatory cytokines that participate in and mediate immune and inflammatory responses. A study by Aiba et al. showed a significant increase in serum levels of TNF-like ligand 1A in patients with PBC, and its levels were significantly decreased after treatment with ursodeoxycholic acid [50]. A study of autoimmune liver disease (including PBC and autoimmune hepatitis) showed that IL-1 $\beta$  and TNF- $\alpha$  levels were significantly increased in patients with autoimmune liver disease [51]. In another article, Donaldson et al. revealed a complex relationship between immunomodulatory genes and PBC. They also showed that the IL-1 gene is a marker of disease susceptibility and progression and that IL-1 $\beta$  plays an important role

in disease [52].

We verified the binding of the significant components in SMF to core targets using a molecular docking method, and the results showed that the receptors and ligands exhibited good binding properties. In addition, the results of in vitro experiments showed that SMF extract significantly improved the viability of HIBEC-EMT cells, reduced the levels of TNF- $\alpha$  and IL-1 $\beta$ , inhibited the inflammatory response, and restored the levels of STAT3, JAK2, Vimentin, and E-cadherin. Therefore, we conclude that SMF may exert a therapeutic effect on the epithelial mesenchymal transition process in PBC by acting on the above important targets and the pathways they are involved in. However, the following limitations of this study exist: 1. In vivo experimental validation in animals was not performed, and lacks mechanistic regulation studies in a real in vivo environment in this study. 2. We investigated the binding of significant components and core targets by molecular docking technique; however, the current results are only at the computer level and lacked experimental validation by experiments such as surface plasmon resonance technique or bio-layer interferometry. 3. The functions of several obtained targets in PBC have not been further investigated, and experiments such as gene knockdown, overexpression, target activation, and inhibition should be applied for in-depth investigation. Therefore, in follow-up work, we will further explore the above issues.

### Conclusion

In this study, we investigated the potential mechanism of action of SMF for the treatment of PBC using network pharmacology, the GEO dataset, and molecular docking techniques and validated it using in vitro experiments. SMF may act on multiple important targets (e.g., STAT3, JAK2, TNF- $\alpha$ , IL-1 $\beta$ , Vimentin, and E-cadherin) and pathways in which they are involved, such as the JAK-STAT, TNF- $\alpha$ , and PI3K-AKT signaling pathways, and thus have a therapeutic impact on the epithelial mesenchymal transition process of PBC. With the help of bioinformatics and in vitro experiments, this study elucidated the potential targets of SMF for the treatment of PBC. The results of this study may provide a theoretical basis for clinical SMF for the treatment of PBC and contribute to the internationalization of the research process of Chinese and Tibetan medicine.

### References

1. Tsuneyama K, Baba H, Morimoto Y, Tsunematsu T, Ogawa H. Primary Biliary Cholangitis: Its Pathological Characteristics and Immunopathological Mechanisms. *J Med Invest* 2017;64(1.2):7–13. Available at: <http://doi.org/10.2152/jmi.64.7>
2. Chasca DMH, Lindor KD. Emerging therapies for PBC. *J Gastroenterol* 2020;55(3):261–272. Available at: <http://doi.org/10.1007/s00535-020-01664-0>
3. Lleo A, Marzorati S, Anaya JM, Gershwin ME. Primary biliary cholangitis: a comprehensive overview. *Hepatol Int* 2017;11(6):485–499. Available at: <http://doi.org/10.1007/s12072-017-9830-1>
4. Lleo A, Leung PSC, Hirschfield GM, Gershwin EM. The Pathogenesis of Primary Biliary Cholangitis: A Comprehensive Review. *Semin Liver Dis* 2019;40(1):34–48. Available at: <http://doi.org/10.1055/s-0039-1697617>
5. Zhang MY, Zhao J, Xie H, Liang QS, Zou ZS, Sun Y. Immune pathogenesis of primary biliary cholangitis. *Chin J Hepatol* 2021;29(6):500–504. Available at: <http://doi.org/10.3760/cma.j.cn501113-20210430-00213>
6. Ma WT, Chen DK. Immunological abnormalities in patients with primary biliary cholangitis. *Clin Sci (Lond)* 2019;133(6):741–760. Available at: <http://doi.org/10.1042/CS20181123>
7. Parés A. Colangitis biliary primaria. *Med Clin (Barc)* 2018;151(6):242–249. Available at: <http://doi.org/10.1016/j.medcli.2017.12.021>

8. Shah RA, Kowdley KV. Current and potential treatments for primary biliary cholangitis. *Lancet Gastroenterol Hepatol* 2020;5(3):306–315. Available at: [http://doi.org/10.1016/S2468-1253\(19\)30343-7](http://doi.org/10.1016/S2468-1253(19)30343-7)
9. Carino A, Biagioli M, Marchianò S, et al. Opposite effects of the FXR agonist obeticholic acid on Mafg and Nrf2 mediate the development of acute liver injury in rodent models of cholestasis. *Biochim Biophys Acta Mol Cell Biol Lipids* 2020;1865(9):158733. Available at: <http://doi.org/10.1016/j.bbali.2020.158733>
10. Firrincieli D, Boissan M, Chignard N. Epithelial-mesenchymal transition in the liver. *Gastroenterol Clin Biol* 2010;34(10):523–528. Available at: <http://doi.org/10.1016/j.gcb.2010.04.017>
11. Pan Y, Wang J, He L, Zhang F. MicroRNA-34a Promotes EMT and Liver Fibrosis in Primary Biliary Cholangitis by Regulating TGF- $\beta$ 1/smad Pathway. *J Immunol Res* 2021;2021:6890423. Available at: <http://doi.org/10.1155/2021/6890423>
12. Robertson H, Kirby JA, Yip WW, Jones DEJ, Burt AD. Biliary epithelial-mesenchymal transition in posttransplantation recurrence of primary biliary cirrhosis. *Hepatology* 2007;45(4):977–981. Available at: <http://doi.org/10.1002/hep.21624>
13. Zhao YL, Zhu RT, Sun YL. Epithelial-mesenchymal transition in liver fibrosis. *Biomed Rep* 2016;4(3):269–274. Available at: <http://doi.org/10.3892/br.2016.578>
14. Liu R, Li X, Huang N, Fan M, Sun R. Toxicity of traditional Chinese medicine herbal and mineral products. *Adv Pharmacol* 2020;301–346. Available at: <http://doi.org/10.1016/bs.apha.2019.08.001>
15. Zhao Y, Yang A, Tu P, Hu Z. Anti-tumor effects of the American cockroach, *Periplaneta americana*. *Chin Med* 2017;12(1):26. Available at: <http://doi.org/10.1186/s13020-017-0149-6>
16. Yun H, Duan X, Xiong W, et al. Exploration of the Hepatoprotective Effect and Mechanism of *Swertia mussoitii* Franch in an Acute Liver Injury Rat Model. *Comb Chem High Throughput Screen* 2020;22(9):649–656. Available at: <http://doi.org/10.2174/1386207322666191106105725>
17. Yun H, Wu X, Ding Y, et al. Exploring the Mechanism of *Swertia mussoitii* Franch. for Hepatoprotective Effects with iTRAQ LC-MS/MS. *Comb Chem High Throughput Screen* 2021;24(9):1332–1339. Available at: <http://doi.org/10.2174/1386207323666201020111301>
18. Tian C, Zhang T, Wang L, Shan Q, Jiang L. The hepatoprotective effect and chemical constituents of total iridoids and xanthenes extracted from *Swertia mussoitii* Franch. *J Ethnopharmacol* 2014;154(1):259–266. Available at: <http://doi.org/10.1016/j.jep.2014.04.018>
19. Wang H, Yuan X, Huang H, Zhang B, Cao C, Zhao HP. Chemical constituents from *Swertia mussoitii* Franch. (Gentianaceae). *Nat Prod Res* 2017;31(14):1704–1708. Available at: <http://doi.org/10.1080/14786419.2017.1286480>
20. Chai J, Du X, Chen S, et al. Oral administration of oleanolic acid, isolated from *Swertia mussoitii* Franch, attenuates liver injury, inflammation, and cholestasis in bile duct-ligated rats. *Int J Clin Exp Med* 2015;8(2):1691–1702. Available at: <http://www.ncbi.nlm.nih.gov/pmc/articles/PMC4402745>
21. Contreras-Omaña R, Velasco JV-R, Castro-Narro G, et al. Approach to the patient with cholestasis and jaundice syndrome. Joint AMH, AMG, and AMEG scientific position statement. *Rev Gastroenterol Mex (Engl Ed)* 2022;87(1):80–88. Available at: <http://doi.org/10.1016/j.rgm.2021.04.003>
22. Sun H, Yang L, Li M, et al. UPLC-G2Si-HDMS untargeted metabolomics for identification of metabolic targets of Yin-Chen-Hao-Tang used as a therapeutic agent of dampness-heat jaundice syndrome. *J Chromatogr B Analyt Technol Biomed Life Sci* 2018;1081–1082:41–50. Available at: <http://doi.org/10.1016/j.jchromb.2018.02.035>
23. Si MD, Wu M, Cheng XZ, et al. *Swertia mussoitii* prevents high-fat diet-induced non-alcoholic fatty liver disease in rats by inhibiting expression of the TLR4/MyD88 and the phosphorylation of NF- $\kappa$ B. *Pharm Biol* 2022;60(1):1960–1968. Available at: <http://doi.org/10.1080/13880209.2022.2127153>
24. Zhang L, Cheng Y, Du X, et al. *Swertia mussoitii* Franch, an Herbal Agent Derived from *Swertia mussoitii* Franch, Attenuates Liver Injury, Inflammation, and Cholestasis in Common Bile Duct-Ligated Rats. *Evid Based Complement Alternat Med* 2015;2015:948376. Available at: <http://doi.org/10.1155/2015/948376>
25. Dai Y. Study on the chemical constitutions of the ethyl acetate extract from *swertia mussoitii*. 2018;10:90. (Chinese) Available at: [https://kns.cnki.net/kcms2/article/abstract?v=Pk5Eu7LuuI64xwCr7ays1TwTnpbeG4I7hn0V3tLqfN-spPgXNQOrJQAhhqWUGLN8-nJ3uuWoZYuoYXj2V1QIwIQIGnRSJyDW41b0Rzd3vHaLzBKA8OGy0lvYuUFYv9Mby4gqEr\\_3g=&uniplatform=NZKPT&language=CHS](https://kns.cnki.net/kcms2/article/abstract?v=Pk5Eu7LuuI64xwCr7ays1TwTnpbeG4I7hn0V3tLqfN-spPgXNQOrJQAhhqWUGLN8-nJ3uuWoZYuoYXj2V1QIwIQIGnRSJyDW41b0Rzd3vHaLzBKA8OGy0lvYuUFYv9Mby4gqEr_3g=&uniplatform=NZKPT&language=CHS)
26. Buntrock RE. ChemOffice Ultra 7.0. *J Chem Inf Comput Sci* 2002;42(6):1505–1506. Available at: <http://doi.org/doi:10.1021/ci025575p>
27. Daina A, Michielin O, Zoete V. SwissADME: a free web tool to evaluate pharmacokinetics, drug-likeness and medicinal chemistry friendliness of small molecules. *Sci Rep* 2017;7(1):42717. Available at: <http://doi.org/10.1038/srep42717>
28. Baell JB, Holloway GA. New Substructure Filters for Removal of Pan Assay Interference Compounds (PAINS) from Screening Libraries and for Their Exclusion in Bioassays. *J Med Chem* 2010;53(7):2719–2940. Available at: <http://doi.org/10.1021/jm901137j>
29. Daina A, Michielin O, Zoete V. SwissTargetPrediction: updated data and new features for efficient prediction of protein targets of small molecules. *Nucleic Acids Res* 2019;47(W1):W357–W364. Available at: <http://doi.org/10.1093/nar/gkz382>
30. Liu X, Ouyang S, Yu B, et al. PharmMapper server: a web server for potential drug target identification using pharmacophore mapping approach. *Nucleic Acids Res* 2010;38(Web Server issue):W609–W614. Available at: <http://doi.org/10.1093/nar/gkq300>
31. Wang X, Pan C, Gong J, Liu X, Li H. Enhancing the Enrichment of Pharmacophore-Based Target Prediction for the Polypharmacological Profiles of Drugs. *J Chem Inf Model* 2016;56(6):1175–1183. Available at: <http://doi.org/10.1021/acs.jcim.5b00690>
32. Wang X, Shen Y, Wang S, et al. PharmMapper 2017 update: a web server for potential drug target identification with a comprehensive target pharmacophore database. *Nucleic Acids Res* 2017;45(W1):W356–W360. Available at: <http://doi.org/10.1093/nar/gkx374>
33. Stelzer G, Rosen N, Plaschkes I, et al. The GeneCards Suite: From Gene Data Mining to Disease Genome Sequence Analyses. *Curr Protoc Bioinformatics* 2016;54(1):1.30.1–1.30.33. Available at: <http://doi.org/10.1002/cpbi.5>
34. Amberger JS, Hamosh A. Searching Online Mendelian Inheritance in Man (OMIM): A Knowledgebase of Human Genes and Genetic Phenotypes. *Curr Protoc Bioinformatics* 2017;58(1):1.2.1–1.2.12. Available at: <http://doi.org/10.1002/cpbi.27>
35. Szklarczyk D, Gable AL, Nastou KC, et al. The STRING database in 2021: customizable protein–protein networks, and functional characterization of user-uploaded gene/measurement sets. *Nucleic Acids Res* 2020;49(D1):D605–D612. Available at: <http://doi.org/10.1093/nar/gkaa1074>

36. Zhou Y, Zhou B, Pache L, et al. Metascape provides a biologist-oriented resource for the analysis of systems-level datasets. *Nat Commun* 2019;10(1):1523. Available at: <http://doi.org/10.1038/s41467-019-09234-6>
37. Shannon P, Markiel A, Ozier O, et al. Cytoscape: A Software Environment for Integrated Models of Biomolecular Interaction Networks. *Genome Res* 2003;13(11):2498–2504. Available at: <http://doi.org/10.1101/gr.1239303>
38. Hardie C, Green K, Jopson L, et al. Early Molecular Stratification of High-risk Primary Biliary Cholangitis. *EBioMedicine* 2016;14:65–73. Available at: <http://doi.org/10.1016/j.ebiom.2016.11.021>
39. Smyth GK. Linear Models and Empirical Bayes Methods for Assessing Differential Expression in Microarray Experiments. *Stat Appl Genet Mol Biol* 2004;3(1):Article3. Available at: <http://doi.org/10.2202/1544-6115.1027>
40. Trott O, Olson AJ. AutoDock Vina: Improving the speed and accuracy of docking with a new scoring function, efficient optimization, and multithreading. *J Comput Chem* 2009;31(2):455–461. Available at: <http://doi.org/10.1002/jcc.21334>
41. Pellicciari R, Fiorucci S, Camaioni E, et al. 6alpha-ethyl-chenodeoxycholic acid (6-ECDC), a potent and selective FXR agonist endowed with anticholestatic activity. *J Med Chem* 2002;45(17):3569–3572. Available at: <http://doi.org/10.1021/jm025529g>
42. Gulamhusein AF, Hirschfield GM. Primary biliary cholangitis: pathogenesis and therapeutic opportunities. *Nat Rev Gastroenterol Hepatol* 2019;17(2):93–110. Available at: <http://doi.org/10.1038/s41575-019-0226-7>
43. Cordell HJ, Fryett JJ, Ueno K, et al. An international genome-wide meta-analysis of primary biliary cholangitis: Novel risk loci and candidate drugs. *J Hepatol* 2021;75(3):572–581. Available at: <http://doi.org/10.1016/j.jhep.2021.04.055>
44. Trivedi PJ, Cullen S. Etiopathogenesis of primary biliary cirrhosis: an overview of recent developments. *Hepatol Int* 2012;7(1):28–47. Available at: <http://doi.org/10.1007/s12072-012-9362-7>
45. Jung K, Kim M, So J, Lee S, Ko S, Shin D. Farnesoid X Receptor Activation Impairs Liver Progenitor Cell-Mediated Liver Regeneration via the PTEN-PI3K-AKT-mTOR Axis in Zebrafish. *Hepatology* 2021;74(1):397–410. Available at: <http://doi.org/10.1002/hep.31679>
46. Xiao Y, Wang J, Chen Y, et al. Up-regulation of miR-200b in biliary atresia patients accelerates proliferation and migration of hepatic stellate cells by activating PI3K/Akt signaling. *Cell Signal* 2014;26(5):925–932. Available at: <http://doi.org/10.1016/j.cellsig.2014.01.003>
47. Wu X, Zheng X, Wen Q, et al. Swertia cincta Burkill alleviates LPS/D-GalN-induced acute liver failure by modulating apoptosis and oxidative stress signaling pathways. *Aging (Albany NY)* 2023;15(12):5887–5916. Available at: <http://doi.org/10.18632/aging.204848>
48. Zhang Q, Chen K, Wu T, Song H. Swertiamarin ameliorates carbon tetrachloride-induced hepatic apoptosis via blocking the PI3K/Akt pathway in rats. *Korean J Physiol Pharmacol* 2019;23(1):21. Available at: <http://doi.org/10.4196/kjpp.2019.23.1.21>
49. Cao H, Zhu B, Qu Y, Zhang W. Abnormal Expression of ER $\alpha$  in Cholangiocytes of Patients With Primary Biliary Cholangitis Mediated Intrahepatic Bile Duct Inflammation. *Front Immunol* 2019;10:2815. Available at: <http://doi.org/10.3389/fimmu.2019.02815>
50. Aiba Y, Harada K, Komori A, et al. Systemic and local expression levels of TNF-like ligand 1A and its decoy receptor 3 are increased in primary biliary cirrhosis. *Liver Int* 2013;34(5):679–688. Available at: <http://doi.org/10.1111/liv.12296>
51. Abe K, Takahashi A, Fujita M, et al. Dysbiosis of oral microbiota and its association with salivary immunological biomarkers in autoimmune liver disease. *PLoS One* 2018;13(7):e0198757. Available at: <http://doi.org/10.1371/journal.pone.0198757>
52. Donaldson P, Agarwal K, Craggs A, Craig W, James O, Jones D. HLA and interleukin 1 gene polymorphisms in primary biliary cirrhosis: associations with disease progression and disease susceptibility. *Gut* 2001;48(3):397–402. Available at: <http://doi.org/10.1136/gut.48.3.397>